Disclaimer

This note has not been internally reviewed by the DØ Collaboration. Results or plots contained in this note were only intended for internal documentation by the authors of the note and they are not approved as scientific results by either the authors or the DØ Collaboration. All approved scientific results of the DØ Collaboration have been published as internally reviewed Conference Notes or in peer reviewed journals.

DØ note 932

2/15/90

COMMENTS ON THE CALIBRATION OF DO CALORIMETER AND THE FEASIBILITY OF THE LOW MOMENTUM HADRON BEAM AT FNAL

H.Piekarz

The Florida State University, Tallahassee FL32306

1. PHYSICS MOTIVATION

The calorimeters are designed to measure the total energy released in the high-energy interaction. The released energy propagates through the calorimeter mostly in the form of the electromagnetic and hadronic showers. In compliance with this characteristic feature of the high-energy interactions the calorimeter detectors are constructed in such a way as to be efficient to either of the two showers, providing their identity, energy and charged particle multiplicity.

Due to strong fragmentation processes [1] occuring at the high-energy reactions the momentum spectra of the emitted particles are very broad with the low momentum end being at the calorimeter threshold energy, typically a fraction of a GeV, and the high momentum end ranging values higher than 100 GeV/c. Based on the UA's and CDF data one observes that e.g. a substantial amount of the charged jet energy is released through emission of particles (pions) of momenta lower than 10 GeV/c.

Typically for the jet event of Et=70 GeV there is (40-60)% probability that the emitted charged pions have momenta below 10 GeV/c and (10-20)% chance that the particle momenta are below 2 GeV/c .

With decrease of the jet energy the low momentum pions constitute even higher fraction of the released charged energy. Consequently, as low as possible energy cut should be used in the analysis of the calorimeter events and the response to both, electrons and hadrons must be measured or predicted for the entire energy range.

Complexity of the calorimeter structure combined with diversity of the physics processes of particle energy loss as the momentum changes, make the predictions of the calorimeter response rather difficult. The Monte-Carlo simulation of that response requires experimental input at wide range of particle momenta as well as at variety of the calorimeter locations including cracks and other non-uniformities, where the energy loss is not well accountable.

Based on the above we conclude that the studies of the calorimeter response and the signal-energy calibration must be done using the beam of electrons and hadrons of broad momentum range. Those beams should also have rates allowing for hundreds of calorimeter spots to be examined. In addition the calorimeter simulation studies should preceed the experimental tests in order to identify locations best suitable for tuning the simulation programs.

For electrons or positrons of momentum greater than 0.1 GeV/c the energy loss is almost entirely through bremsstrahlung. This homogeneouty

of electron interactions (regardless the beam momentum) causes that the response to electrons is expected to be linear. Consequently, the measurements at the high momentum end (where the electron beams are more easily available) combined with the detector electronics calibration (using e.g. charge injection) may provide satisfactory information on the calorimeter response to electrons.

In the case of the hadron beams a linear response of calorimeter is less likely to be observed. The CDF calibration data [2] for pions in the momentum range of 0.5 GeV/c up to 150 GeV/c (Fig.1) indicate that the response is strongly unlinear below some 20 GeV/c hadron momentum.

Tha CDF data are presented in the form of a ratio of the measured energy in the calorimeter over the momentum of the same particle seen in the magnetic spectrometer. Based on the measured particle momentum the calorimeter signal is smaller than expected. The deviation strongly increases at lower momenta and the calorimeter defficiency reaches almost 50% value at about 1 GeV.

It is interesting to point out that the energy defficiency of the CDF calorimeter can be divided into three rather distinguishable energy intervals. The first one is for the energies below 1 GeV/c, second extends from above 1 GeV up to about 15 GeV and the third one is above 15 GeV. In each of these intervals we observe rather linear change of the response with the LogE value of particle energy. Although at present we do not have an understanding of this effect, one should look for such regularities as they may allow to project and fit more accurately the calorimeter response to hadronic beams. The calorimeter response depends on the details of the

calorimeter structure, such as type of absorber, ratio of the active to nonactive layers, electronic noise, etc. and therefore the DO calorimeter may have its deficiency of the response at low particle momenta quite different than that of the CDF or other calorimeters.

Some of the DO calorimeter modules were exposed to beams of pions and electrons and the results were recently published [3]. As the response to an electron beam is expected to be linear the ratio of the electron over the pion amplitude as a function of beam momentum is a good measure of the the calorimeter nonlinearity to hadrons.

The e/pi ratio for the DO calorimeter module as a function of the beam momentum is shown in Fig.2, where the results from the HELIOS [4] Uranium/ liquid argon calorimeter are also presented for comparison. In the HELIOS calorimeter the signal was integrated over two different time intervals; 100 ns and 250 ns. In the DO calorimeter the charge collection time is 2000 ns. Both, the DO and HELIOS data indicate that the e/pi value decreases with hadron energy. With the 250 ns integration time the e/pi ratio of HELIOS calorimeter gets smaller than 1 above 400 GeV. For the DO calorimeter this happens above 120 GeV. Based on the CDF calibration (Fig.1) we expect the e/pi ratio to have its maximum at about 1 GeV. Below this energy it will probably decrease again.

Interesting result came out recently from the ZEUS [5] experiment where it was found that protons and pions have the same response if presented as a function of the beam kinetic energy instead of momentum (Fig.3 and 4). These results indicate that both, protons and pions can be used interchangeably for calorimeter calibration. The above figures also show, however, how strong is the change of the e/h ratio and the resolution at low energies.

The DO data were measured with long integration time and also in the momentum region (> 20 GeV/c) in which the compensation factor is closest to unity in most of calorimeters. We expect, however, that for the DO calorimeter the momentum dependence of the e/h ratio is as strong as in other experiments.

Summary:

As at present there are no DO calorimeter data for the energy range below 20 GeV we conclude that a strong effort should be made in order to measure the hadron energy detection efficiency in this low energy region.

The linearity measurements with low energy electrons are also of great importance so the physics and electronics effects can be compared and shed even more light on the hadronic response.

In addition high statistics measurements should be made at energies above 20 GeV for both, electrons and pions. The deviation from the linearity in the high energy region may help to understand the defficiencies at lower energies and help to establish guidelines for the Monte-Carlo simulation of the calorimeter response in the entire energy range.

In the following chapters the feasibility of the low momentum hadronic beam for the DO Calorimeter test will be discussed. The projected hadronic fluxes at momenta below 5 GeV/c will be presented.

2. OUTLINE OF THE SCHEME FOR THE LOW MOMENTUM BEAM AT NW LINE

The secondary beam particles (pions) in the NW line are produced from the interaction of the 800 GeV/c protons in the primary target located at Z=4600, which is 580 m away from the experimental area in NWA. The length of the beam line is the most important single factor limiting the flux of the low momentum (less than 2 GeV/c) secondary pions in the NWA area as very few such pions can survive this long flight path.

High transmission loss at low momenta (see next chapter) is a second most important factor limiting pion beams and also low momentum proton beams in the NW line.

Consequently, the low momentum hadrons should be produced as close as possible to the experimental area in NWA. As it is not possible to send the primary proton beam down the NW line the secondary beam of momentum (30-200) GeV/c must be used for producing the tertiary beams of momenta below 5 GeV/c.

The schematic diagram of the NW line is shown in Fig.5. The target for the tertiary beam has to be located in the area which fulfills the radiation safety requirements (3 feet of berm for maximum of E8 beam particles). The area of the NW8 (Fig.6) is the closest location to NWA with more than 3 feet of berm (Fig.7). Incidently, the spectrometer part of the NW beam line starts in the NW8, so the momentum of the tertiary beam can be measured using the same setup as for the secondary beam. The distance of the tertiary target to the experimental area in NWA is 140m.

This continues to be a long distance for pions of momenta below 2 GeV/c. Therefore if the progress in improvement of the secondary beams turns out to be unsatisfactory one should consider a production of the tertiary beams in NWA area. This solution, however, has high potential for radiation problems as well as increased difficulty in particle/momentum identification.

3. PRODUCTION OF THE SECONDARY BEAMS IN THE NW LINE

The NW line exists since 1978 when it was first used for the production of neutrinos. From early 1980's it was basically used for producing the pion and electron beams for calibration of the collider detectors (CDF and DO).

The typically observed pion and electron rates per 800 GeV/c proton are shown in Fig.8 . As the rate of the incident protons is in average (3-5)xE11 per spill the secondary beam fluxes are satisfactory down to some 20 GeV/c of the pion momentum.

In order to produce the tertiary beam, however, it is indispensible to have the intensity of the secondary beam as high as possible. Therefore we decided to investigate if the intensity of the secondary beams in the NW line was optimal.

Knowing the pion production cross-section, the beam line solid angle and percentage of momentum acceptance one can project the secondary beam rates. A comparison of these rates with observed ones will give the value of the actual beam transmission and its dependence on the momentum.

The pion production in proton-proton collisions has been extensively studied in the past [6,7] giving the empirical formulae comprising the primary beam momentum up to TeV range and the secondary beam momentum down to a fraction of GeV/c. The momentum dependent scaling cross-section law allows one to predict with reasonable credibility the cross-section for almost any pion producing p + p --> Pi + "anything" reaction. In addition it has been also found that the p + p cross-sections can be used for the p + nucleus as well as Pi + nucleus reactions, both scaling with momentum. The Pi- + p (nucleus) --> Pi- + "anything" reactions have typically cross sections about (0.5-0.7) of the corresponding p + p reaction. In addition the production of the negative pions in p + p reaction is about (0.5-0.7) of the production of the positive pions.

In Fig.9 we present the estimated cross-sections for the negative pion production by the 800 GeV/c protons. These cross-sections were obtained by averging the cross-sections given in [6] for the 500 and 1100 GeV/c proton induced reactions (the momentum-weight averaging gives some 10% higher cross-sections). As expected these cross-sections scale almost linearly with secondary beam momentum as long as its value is a small fraction (< 10%) of the momentum of the primary beam. Those cross-sections are presented for the 0 deg. production angle which gives the highest cross-section value at any secondary beam momentum. The production of the positive pions is about a factor two higher than negatives. In order to avoid background from the primary protons typically the negative pions are transmitted in the NW beam line.

The first focusing quadrupoles in the NW line are located at an average distance of 106.4m from the production target. They have 3" (7.5 cm) aperture

which allows for a maximum solid angle acceptance of about E-6 sr.

Assuming the cross-sections given in Fig.9, the beam line solid angle acceptance E-6 sr, momentum acceptance 2% and 30 cm (1 coll. length) Al production target we can calculate the expected negative pion fluxes in the NW beam line. The beam rates at the NWA experimental target must be corrected for the pion decay losses on the 580m flight path. The summary of this investigation is presented in Table 1.

The observed negative pion production rates are much lower than the predicted value. At the medium momentum of the secondary beam ((70-100) GeV/c) the measured pion flux is about 5% of the optimal value. Obtained in this way NW beam line acceptance is shown in Fig.10. One can see that at both, the high and low momentum end the beam particles are not transported.

There is certainly an error in the projected value of the cross-section for the pion production and there is also an error in the estimated value of the solid angle acceptance (although the calculations using TURTLE [8] agree with the value of E-6 sr estimated solid angle) for the NW beam line. In spite of those errors, however, one can state that the pion fluxes in the NW line are at least an order of magnitude too low.

Following the above conclusion we requested a check of the alignment of the decay beam pipe as a primary suspect for the obstruction of the beam. The NW beam line is 580 m long with about 305.3 m of a decay pipe. Most of this pipe is about 30 cm in diameter and is burried in the ground without any solid support, which makes it vulnurable to dislocations.

The decay pipe of the NW beam line was surveyed in 1978 and showed then

dislocations but not large enough to cause the interaction with the assumed 7-8 cm beam spot size. The recent survey showed, however, that in the section pipe between the NW5 and NW6 enclosures there was a vertical shift of the pipe by more than 14 cm (Fig.11). As the pipe diameter is 30 cm this obstacle may cause some 50% of the beam loss assuming that the remaining parts of the beam line are well aligned and that there is no correlation between the obstructed beam phase space and the most accepted beam phase space in downstream sections of the beam line.

The beam steering by faulting magnetic elements is often found as an important reason for the beam intensity loss. This may happen for example when there is a current short in the magnet. Small shorts are not always detectable. A careful measurement of the actual distribution of the magnetic field is needed to find them. With large distances between the magnets in the NW line even a small steering could lead to large beam losses.

The most probable cause, however, of the peculiar momentum dependent acceptance of the NW line is poor regulation of magnet power supplies which allows for transmission of particles at a certain momentum range where either the regulation is most stable or least important. In such a case the beam intensity loss will occur most likely at the beam bends. There are 4 bends in NW beam line (4W, 6E, 7W and 9E). In Fig.12 we present the 100 GeV/c negative pion beam intensity loss observed at each bend. This loss is presented as a function of a distance to the production target. We find that the larger is this distance the higher intensity loss is observed. From the Fig.12 we estimate that total beam intensity loss on the bends is equal to:

$$0.22 = 0.90(4W) \times 0.73(6E) \times 0.61(7W) \times 0.56(9E)$$

The increased beam intensity loss with a distance to the production target is related to the increased phase space of the beam. Therefore, better beam focalization will not only increase the solid angle but also improve beam transmission. We do not know, however, whether it would produce a radical improvement at momenta which are further away from the medium value.

Some contribution to the beam intensity loss comes from the multiple scatttering on the numerous pipe windows, beam instrumentation and remnents of the gas in the beam pipes. The large distances between the focusing beam elememts in the NW line certainly facilitate the losses due to this effect. In order to evaluate the strength of this effect we listed all beam pipe windows, beam instrumentation, vacuum status of the decay pipes and the gas content of the Cerenkov detectors. Some of these results are shown in Fig.13 a,b,c,d,e. We found, however, that the beam intensity loss due to found material is negligible for pion momenta above 10 GeV/c, so it can not be responsible for the intensity loss at 100 GeV/c.

High beam intensity loss will occur if the production angle of the secondary beam deviates from the 0 deg value. The rate of the 100 GeV/c pionms as a function of the production angle for the 800 GeV/c proton induced reaction is presented in Fig.14 [6]. One can see that the secondary beam intensity loss of an "order of magnitude" would occur with the production angle of about 0.4 deg.. Such a large production angle seems to be very unlikely. Due to extremly long distance of the closest magnets to the target in both, a primary and secondary beam a deviation by the 0.4 deg. would have to result from the misalignment of both beam lines with respect to the production target by about 10 cm. At present, however, the production angle is about about 0.06 deg. [8] which gives intensity loss up to a factor 2.

Assuming known or possible beam intensity losses at 100 GeV/c :

(i) transmission through bends:	0.2
(ii) bent decay pipe:	0.5-0.7
(iii) production angle:	0.5

we obtain for the maximum loss a factor of about 20. This combination of factors illustrates that an agreement within 10% of the predicted and observed beam rate at 100 GeV/c is possible (Table 1).

4. SUGGESTIONS FOR IMPROVEMENT OF THE SECONDARY BEAMS IN NW LINE

Install: 1. 1m/1kGauss dipole at the production target (NW3,z=4600)
2. Two 3Q120 (or 3Q60) quads at closest possible location to production target (NW4,z=4820)

The dipole will allow for zero production angle and quads will increase solid angle acceptance to about 3E-6 sr.

Benefit: Possible increase of the secondary pion fluxes of up to a factor of 2 due to zero deg. production , a factor 3 due to larger solid angle, and probably factor 2 due to improved trnasmission through bends. Total flux increase by about a factor of 12.

In summary, including the factor 1.5 due to a corrected bent decay pipe an improvement by a factor of 18 relative to the 1980's rates should be expected. This would produce 8.7E6 100 GeV/c negative pions per E12 protons.

5. PRODUCTION OF THE TERTIARY BEAMS IN THE NW LINE

Based on the pion production cross-sections presented in [6,7,9] we derive the cross-section values for producing 5,2,1 and 0.5 GeV/c negative pions in (Pi-,P-->Pi-,x) reactions induced by 30,70 and 100 GeV/c pions. In this procedure we assumed that the following approximate cross-section relations are valid:

$$0.7(pp\text{-->}Pi+,x) = (Pi-,p\text{-->}Pi-,x) = (pp\text{-->}Pi-,x)$$

The estimated (Pi-,p-->Pi-,x) cross-sections together with the decay rate of the tertiary pions produced in NW8 or NWA are presented in Tab.2.

For the tertiary beam produced in NW8 we assume the momentum acceptance to be 2% and the solid angle accptance 0.4E-4 sr (from TURTLE). The solid angle determined by the 731.5 cm distance of the tertiary target to the 3Q120 doublet of quadrupoles is 0.5E-4 sr. For the tertiary beam produced in NWA we assume that a minimum 7 m distance between the production target and the calorimeter will be needed giving about the same solid angle acceptance as in the case of NW8. Therefore, apart of the difference in pion decay rate both locations of producing tertiary beam will be considered the same although more advanced arrangement of the retargeting in NWA could produce higher rates (see also discussion in Chapter 8).

Assuming the predicted secondary beam production (Tab.1) and the tertiary

beam cross-sections (Tab.2) we calculate the rates for the 0.5, 1, 2 and 5 GeV/c tertiary negative pions. These rates were produced for the 30,70,100 GeV/c secondary negative pion beams and they are shown in Tab.2 and in Fig.15 to allow extrapolation to the intermediate energies. All rates are given per E12 primary 800 GeV/c protons.

It is interesting to note that higher secondary beam momenta seem to be more effective in producing the low momentum tertiary beam. This is due to the fact that the loss of the secondary beam rate with lowering its momentum is not compensated enough with increased production of the tertiary beam at lower secondary beam momentum.

In order to find some confidence in the predicted rates we shall compare our estimated production of 2 GeV/c pion beam induced by 30 GeV/c pions with the 2 GeV/c negative pion beam induced by 30 GeV/c protons at the AGS.

The AGS beam:

Primary beam momentum:	30 GeV/c
Momentum acceptance:	6%
Solid angle:	1.3E-3 sr
Production angle:	5 deg
Negative pion rate: (before decay)	8E-6

The NW beam (prediction):

Primary beam momentum:	30 GeV/c
Momentum acceptance:	2%
Solid angle:	0.4E-4 sr
Production angle:	0 deg
Negative pion rate: (before decay)	1.9E-7

The BNL beam acceptance is about 90 times higher than the NW tertiary beam but there is a loss of about a factor 3 due to 5 deg. production angle which causes that "effective" BNL acceptance is only 30 times higher. Comparing the rates of secondary pions per interacting proton (or pion):

$$[(8E-6)/30]/(1.9E-7) = 1.4$$

we find that our predicted rate for the NW line is about 40% lower. This is a satisfactory agreement and our predicted rates should be considered as lower limits.

The negative tertiary beams will also have contribution from antiprotons. As antiprotons do not decay they may constitute important fraction of the beam in particular at very low momenta. Based on the extrapolation of the results presented in [9] we project that antiprotons constitute about 2% of the pion production at the same momentum. This value of relative production rate was used in rate calculations of all low momentum antiprotons as well as to estimate the proton's contribution in the positive pion beams.

6. RUNNING TIME WITH THE TERTIARY BEAMS

The number of events per energy spectrum for beam particles does not need to be high. We assume that 200 events provides sufficient statistical weight. Much higher statistics may be required, however,if the examined events reside on the background.

For pion beams the background comes from electrons and muons accompanying

pion decays. The study of the electron and muon contamination in the pion beams in NW line was conducted in 1984. The result is shown in Fig.16. In this study no measurements were done for beam particles below 25 GeV/c. We observe, however, that the Log(muon/Pi) and Log(e/Pi) ratios in the pion beam are linear function of the beam momentum. Therefore, by extending these results down to the low beam momentum end we obtain some information on the muon and electron contamination.

At 1 GeV/c the projected ratio of electron beam over pion beam is about 1 and the muon beam over pion beam is 0.2. With such ratios we find that the electron rejection power in hadron beams should be at least a factor of 100 and muon rejection power at least a factor of 20. However, due to uncertainty of the above projection at low energies the actual rejection power for both, electrons and muons in the pion beams should be much higher.

Muons can be efficiently detected using scintillator detectors located behind an absorber. The beam dump used to stop beam particles can be a part of the muon detection system. The 1 GeV/c muons can penetrate about 2.8 m of concrete. For muons of energies lower than 1 GeV/c the scintillator detectors should be inserted at shorter depth of the dump. For muons of higher energies rather a steel absorber placed behind the dump should be used.

Electrons in the beam can be identified using the two He-filled cerenkov detectors located in the upstream section of NWA. Each of them produces about 4-5 phel per electron beam particle giving satisfactory rejection/identification power.

As we can see from Table 3 and Table 4 pion production is accompanied by emission of heavier hadrons. Both, the negative and positive kaons as well

the protons and antiprotons should be identified and provide corresponding triggers. In particular for beams below 2 GeV/c protons or antiprotons must be identified as they constitute large fraction of the beam. As it was shown in [5] pions, kaons and protons (antiprotons) below 10 GeV/c can be well identified using the combination of TOF (below 2.5 GeV/c) and the pressurized 8m long CO2 cerenkov detector (below 10 GeV/c). The same cerenkov detector was also used to provide electron triggers. If the ID of the hadronic particles below 10 GeV/c is required for DO detector test we propose that pressurized cerenkov detector based on N2, CO2 or heavier gas is considered for installation in NWA. The contribution of protons/antiprotons is most important below 2 GeV/c. One should note that below 2 GeV/c pions and protons can be well seperated using lucite cerenkov detector based on the total internal reflection.

With the proposed above triggering system of hadrons, electrons and muons we assume that 200 pions per spectrum will provide sufficient statistical significance. With this assumption we project the running time with the low momentum pions (or hadrons) produced in NW8 or NWA. The results are presented in Table 3 and in Fig.17. The contribution of antiprotons in negative beam and protons in positive beam is also presented as well as the running time for 1000 events if such statistics will be required by the background conditions.

7. PROTON BEAM FROM NW4

As mentioned in Chapter 1 the ZEUS group has shown that response of their calorimetr to pions and protons was about the same if the results are presented as a function of the beam energy. This means that measurements with protons may allow to predict response to pions and vice versa. In Table 3 we presented the estimated contribution of the antiprotons in negative tertiary beams and

protons in positive ones. Based on the extrapolation of the data presented in [9] for 70 GeV/c proton induced reactions we estimated that the low momentum antiprotons are produced at 2% rate of the negative pion production. This rate was applied for all low momentum (less than 5 GeV/c) antiprotons as well as protons (relative to positive pions). As there are no data for the low-momentum proton production induced by 800 GeV/c protons we used the results obtained from the universal particle production formula [10]. These results are listed in Table 4 together with the production rates for other particles. One finds that the proton production is at 2% rate of the pion production regardless the beam momentum. All the rates in Table 4 are for the 0 deg. production angle.

Based on the above estimated proton production cross-section we calculated the expected rates of the low momentum protons produced in NW4 (Table 5). The rates of these protons in NWA are presented assuming the beam transmission as observed for 70 GeV/c particles as well as the estimated low momentum beam transmission. One can see that unless the NW beam transmission is significantly improved at low momenta the NW4 proton rates are lower than the pion rates from NW8 (in particular if positive beam will be used).

8. TERTIARY BEAM IN NWA

In case the secondary beam will not be improved then the only solution for the low momentum beam would be to produce it in the NWA area.

In the preceeding section we assumed that the solid angle acceptance for the spectrometer would be the same as for targeting in NW8. In fact, however, higher solid angle could be coverd depending on the magnet being

used and the distance from the calorimeter. This should be the subject of a study.

The retargeting in NWA has two major difficulties to overcome. One is connected with the increase of the radiation level in NWA. The target would have to be located inside a solid concrete hat (comparable to the present beam stopper) and therefore it would take about a half of the available space in the south part of NWA. We assume that the "spectrometer" which could be a bending magnet about 1m long would be located inside the shielding space.

Another difficulty is related to the necessary detector and electronic system to provide the tracking information although it may be possible to use the existing test beam chambers (for 0.5 GeV/c particles the deflection in the 1kGauss/1m magnet is about 1.5cm/0.1GeV/c).

In summary, the idea of producing the tertiary beam in NWA requires more studies in order to demonstrate clearly feasibility and cost effectivness relative to the longer running times with beams produced in NW8. The achieved degree of progress with the secondary beam is also essential for the NW8 vs NWA decision.

9. CONCLUSIONS

1. For the pion momenta down to 5 GeV/c a secondary beam produced from the 800 GeV/c proton beam in NW4 is most effective.

2. For the pion momenta between 0.5 and 5 GeV/c a tertiary beam produced by 100-150 GeV/c secondary pion beam in NW8 (or NWA) should be used.

3. For both, low momentum secondary beam (down to 5 GeV/c) and for tertiary beams (below 5 GeV/c) the proposed improvements in chapter 4 have to be implemented in order to make the proposed low-momentum beam studies feasible.

Acknowledgment:

We would like to thank Dr.S. Childress, Dr.H.Haggerty, Dr.G.Koizumi and Dr.A.Malensek for several valuable discussions and Al Guthke for accurate inspection of the NW beam line.

We are also grateful to Dr.P.Grannis and Dr.H.Wahl for comments and support.

REFERENCES

1. G.Arnison et al (UA1 Collaboration), Nucl. Phys. B276 (1986), 253

2. R.Blair et al (CDF Collaboration), 7th Topical Workshop on Proton-Antiproton Collider Physics (1988), 202

3. M.Abolins et al (DO Collaboration) NIM A280 (1989), 36

4. see D.Groom, SSC-227 and DO-888 (1989)

5. A.Andresen et al., (ZEUS Group), DESY 89-149 (1989)

6. C.L.Wang, Phys.Rev.D (1973), 2609

7. A.E.Brenner et al., Phys.Rev.D 26 (1982), 1497

8. Fermilab Research Program Workbook (1989), 18

9. Y.M.Antipov et al., Sov.J.N.P 13 (1971), 78

10. A.Malensek, FN-341, FN-341-A (1981)

TABLE 1

SECONDARY NEGATIVE PION FLUXES IN NWA PER E12 800 GeV/c PROTONS

Sec. beam mom.	$d^2\sigma/d\Omega\,dp$ $(p+p->\pi^-+x)$	Pion survival rate (580m)	Predicted beam flux	Observed and estimated (*) beam transmission	Observed fraction of the predicted beam with known losses included
[GeV/c]	[mb/sr.GeV/c]	[%]		[%]	[%]
200	3250	95	2.9 E7	1.6 (*)	-
150	3000	93	2.0 E7	2.9	46
100	2600	90	1.1 E7	4.4	70
70	2100	86	5.9 E6	5.6	88
30	900	71	9.4 E5	4.5	71
20	500	58	4.5 E5	2.4	38
10	300	36	5.1 E4	1.0	16
5	140	13	4.3 E3	0.4 (*)	-
2	50	0.57	2.7 E1	0.1 (*)	-
1	20	0.00003	3 E-4	0.05 (*)	-
0.5	10	0.000000001	2 E-9	0.01 (*)	-

TABLE 2

PREDICTED TERTIARY BEAM RATES IN NWA FOR THE SECONDAERY BEAM *) RETARGETED IN NW8 OR NWA

Sec. Beam mom.	Ter.beam mom.	$d2\sigma/d\Omega dp$ ($\pi^{\mp}p \rightarrow \pi^{-}+x$)	Pion survival rate		Production rate per sec. beam	Predicted flux per E12 protons	
			NW8 (140m)	NWA (10m)		NW8	NWA
[GeV/c]	[GeV/c]	[mb/sr.GeV/c]	[%]				
30	5	110	61	96	1.3E-5	0.8E1	1.2E1
"	2	80	29	91	0.4E-5	1.1E0	3.2E0
"	1	40	8	84	0.9E-6	7.6E-2	7.6E-1
"	0.5	20	0.7	70	0.2E-6	1.6E-3	1.6E-1
70	5	170	61	96	2.0E-5	0.7E2	1.1E2
"	2	90	29	91	0.4E-5	7.0E0	2.3E1
"	1	45	8	84	0.1E-5	5.0E-1	5.0E0
"	0.5	20	0.7	70	0.2E-6	1.0E-2	1.0E0
100	5	230	61	96	2.7E-5	1.8E2	2.9E2
"	2	100	29	91	0.5E-5	1.5E1	4.7E1
"	1	50	8	84	0.1E-5	1.0E0	1.1E1
"	0.5	20	0.7	70	0.2E-6	2.0E-2	2.0E0

TABLE 3

PREDICTED TERTIARY NEGATIVE AND POSITIVE BEAM RATES PER E12 800 GeV/c PROTONS AND RUNNING TIME PER 2E2 PIONS OR E3 HADRONS *)

NEGATIVE BEAMS

Tertiary beam momentum [GeV/c]	(Pions) (NW8)	(Antiprotons) (NW8)	(Pions) (NWA)	(Antiprotons) (NWA)	Run Time per 2E2 pions [h] (NW8)	[h] (NWA)
5	1.4E2	5E0	2.3E2	5E0	0.02	0.014
2	1.2E1	8E-1	3.8E1	8E-1	0.28	0.08
1	0.8E0	2E-1	0.9E1	2E-1	4.2	0.38
0.5	1.6E-2	5E-2	1.6E0	5E-2	210	2.1

POSITIVE BEAMS

Tertiary beam momentum [GeV/c]	(Pions) (NW8)	(Protons) (NW8)	(Pions) (NWA)	(Protons) (NWA)	Run time per 2E2 pions [h] (NW8)	[h] (NWA)	Run time per E3 hadrons [h] (NW8)	[h] (NWA)
5	2.8E2	5E0	4.6E2	E1	0.012	0.008	0.06	0.04
2	2.4E1	1.6E0	7.6E1	1.6E0	0.14	0.044	0.66	0.21
1	1.6E0	4E-1	1.8E1	4E-1	2.1	0.186	8.4	0.91
0.5	3.2E-2	9E-2	3.2E0	E-1	105	1.05	140	5.09

*) The 18-fold increase of intensity of the secondary 100 GeV/c beam flux relative to the 80's rates was assumed (Chapter 4).

TABLE 4

RATES OF LOW MOMENTUM PARTICLES PRODUCED BY E12 800 GeV/c PROTONS *)

MOMENTUM	SECONDARY PARTICLES					
[GeV/c]	PI+	PI-	K+	K-	P+	P-
5	7.8E4	3.5E4	6.7E3	5.5E3	1.6E3	2.3E3
2	1.4E4	5.9E3	1.1E3	1.0E3	3.0E2	4E2
1	3.6E3	1.5E3	2.8E2	2.6E2	7.7E1	E2

*) No particle decay or transmission loss included

TABLE 5

ESTIMATED RATES OF LOW ENERGY PROTONS IN NWA PRODUCED BY E12 PRIMARY 800 GeV/c PROTONS IN NW4

Beam momentum [GeV/c]	Positive pion production rate	Proton production rate	Rates with transmission as for 70 GeV/c beam	Rates with estimated low momentum transmission
5	6.6E4	1.3E3	7.2E1	5.2E0
2	9.4E3	1.9E2	1.1E1	2E-1
1	2E3	4E1	2.2E0	2E-2
0.5	4E2	8E0	0.5E0	0.8E-3

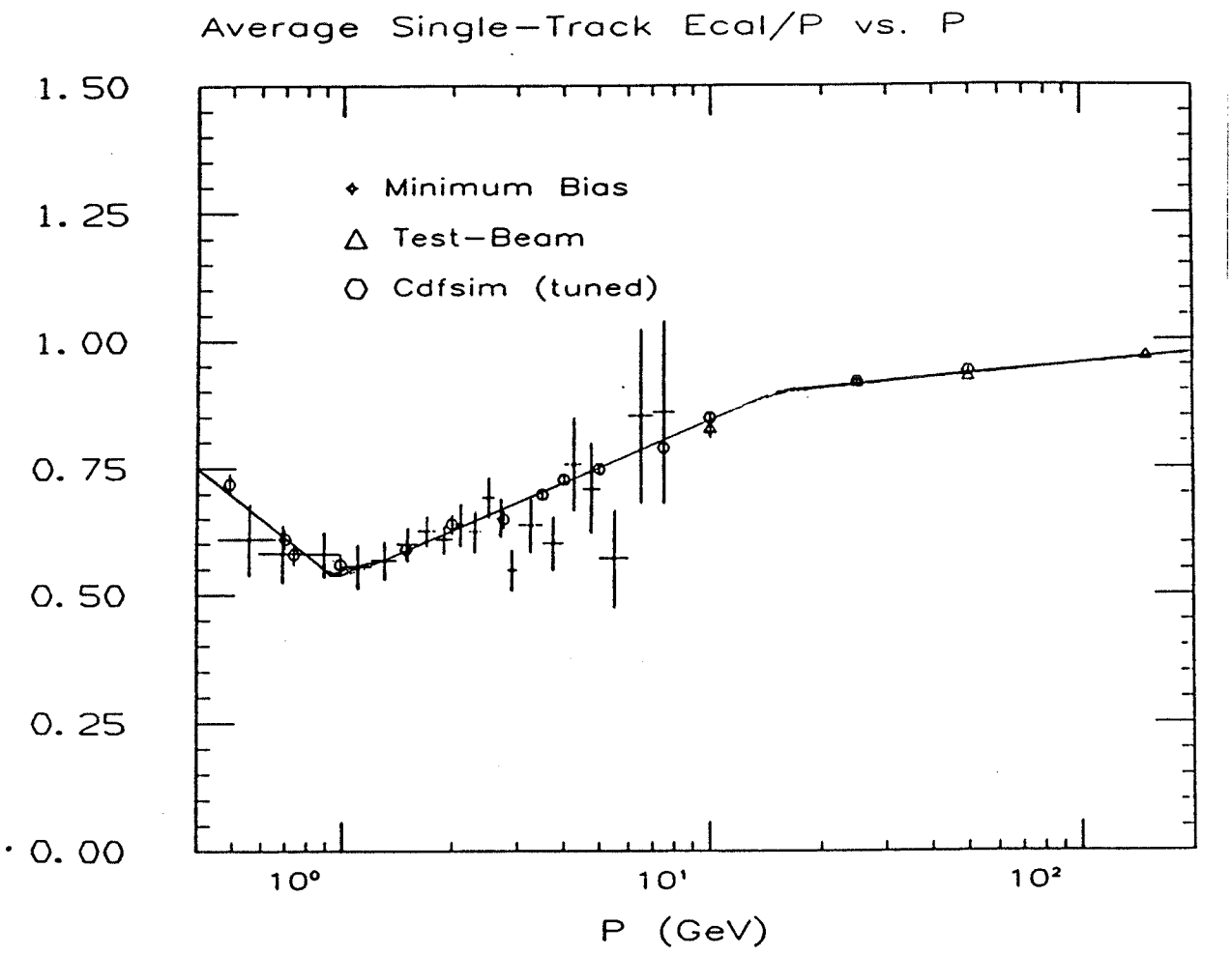

Fig.1 The CDF calorimeter calibration data; the measured ratio of calorimeter response to the true particle momentum.

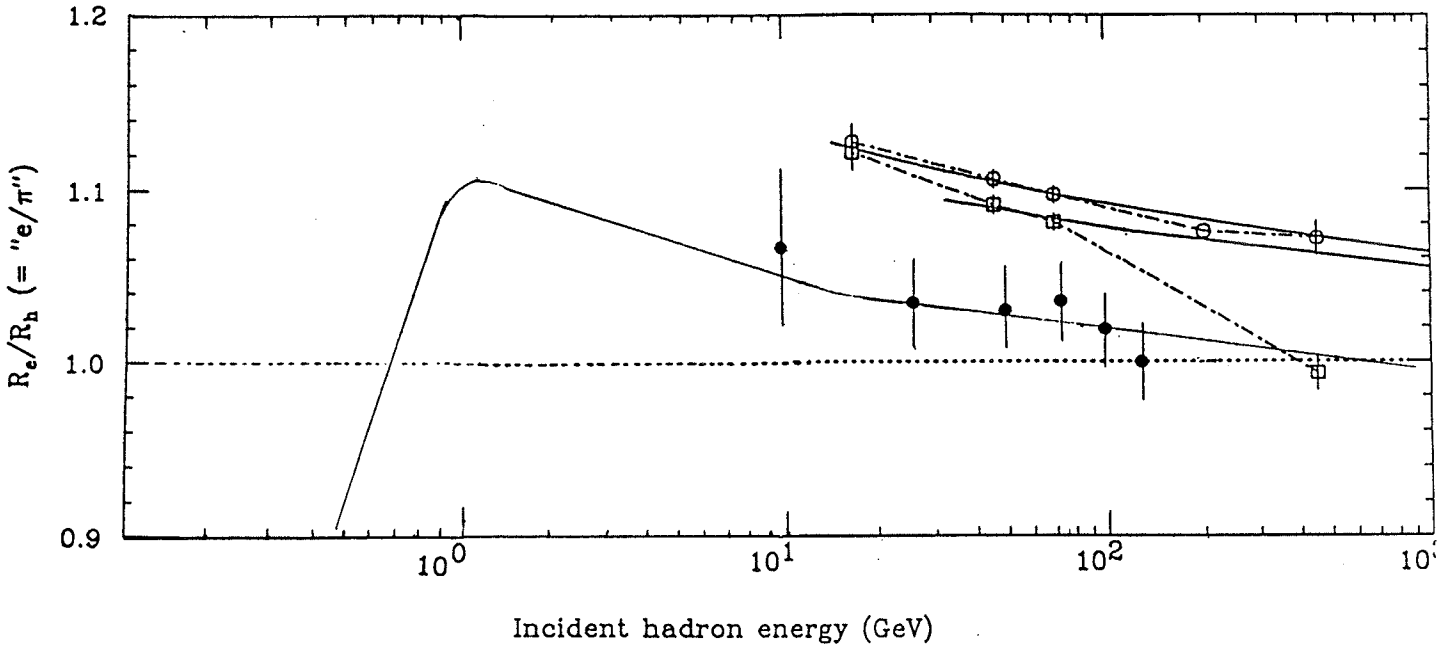

Fig.2 Signal ratio of electrons over pions for U/LAr calorimeters.

○ - HELIOS 100 ns integration

□ - HELIOS 250 ns "

●_ DO 2000 ns "

The solid line for DO data represents the three hadron detection efficiency intervals observed with the CDF calorimeter.

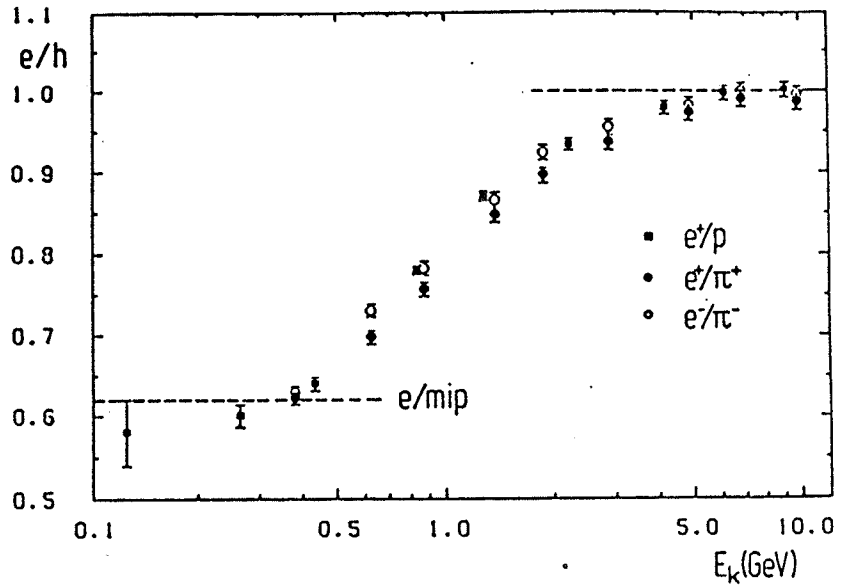

Fig.3 e/h as a function of the kinetic energy for protons and pions. The electron values have been scaled assuming a perfect linearity of the calorimeter response and the hadron values have been corrected for energy losses in front of the calorimeter.

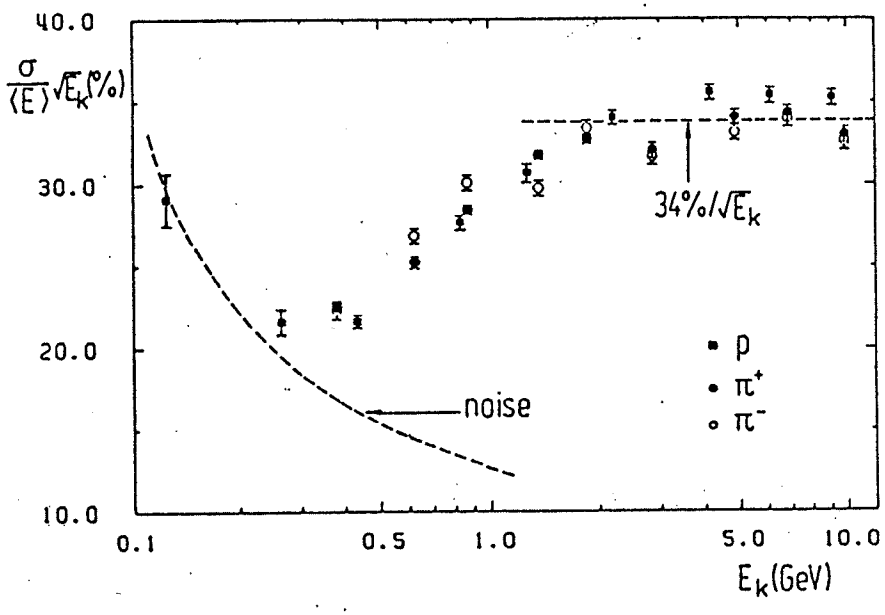

Fig.4 Energy resolution for hadrons as a function of the kinetic energy. The total calorimeter noise is indicated.

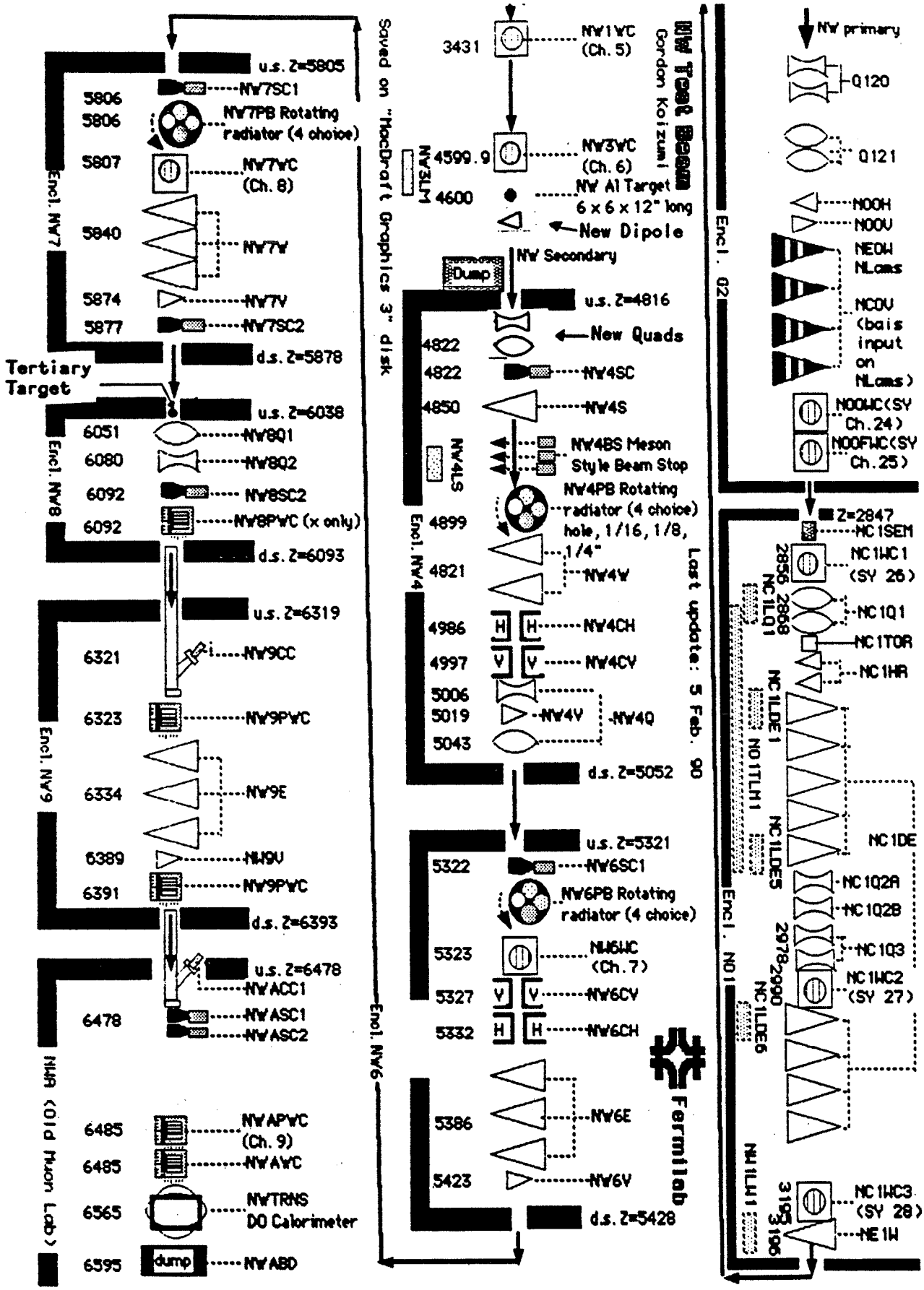

Fig.5 Schematic diagram of the NW beam line.

The proposed position of the new dipole and quads at the secondary beam production target and the location of tertiary beam production target in NW8 are also shown.

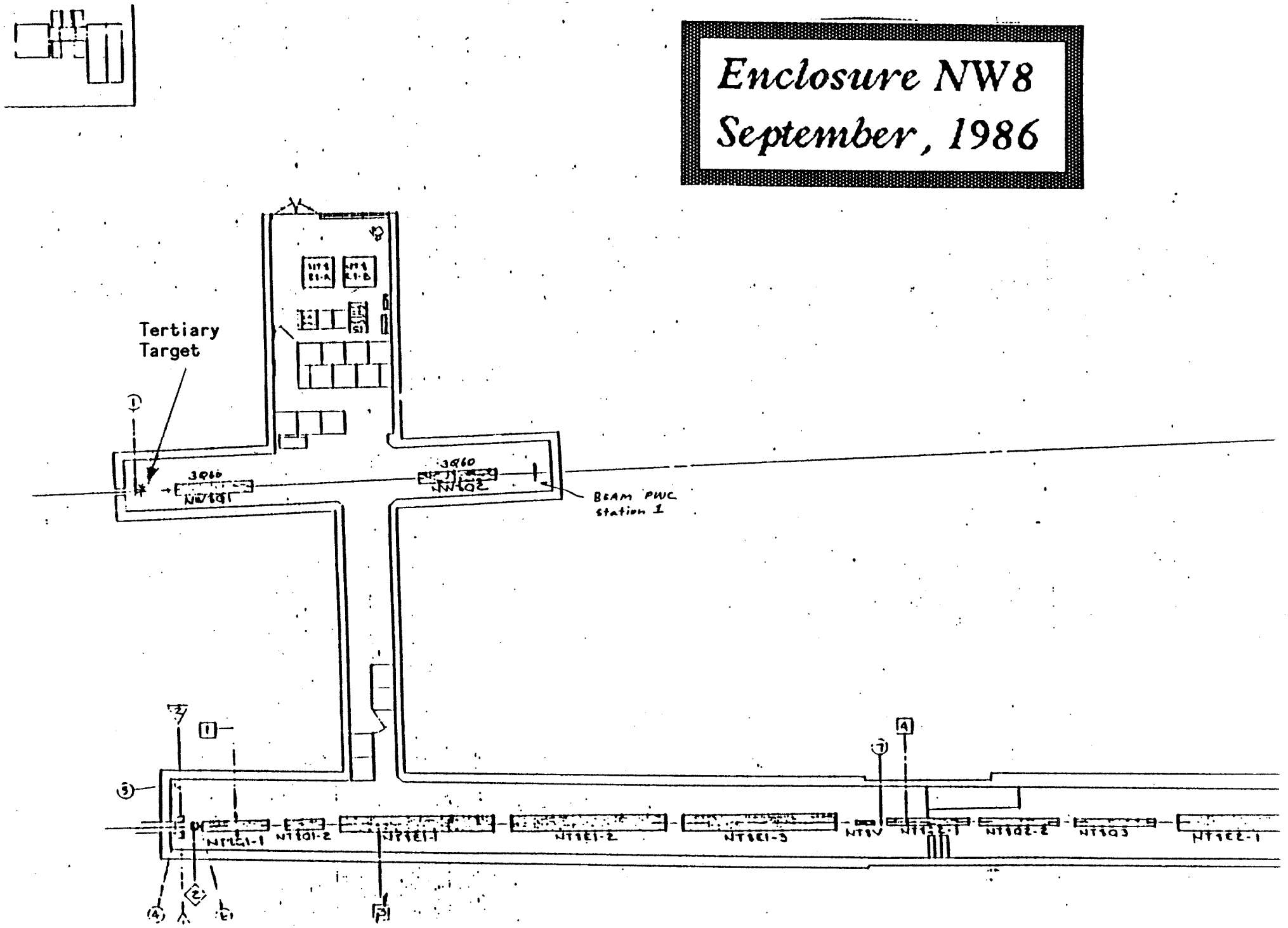

Fig.6 The NW8 enclosure and the proposed location of the tertiary beam target station.

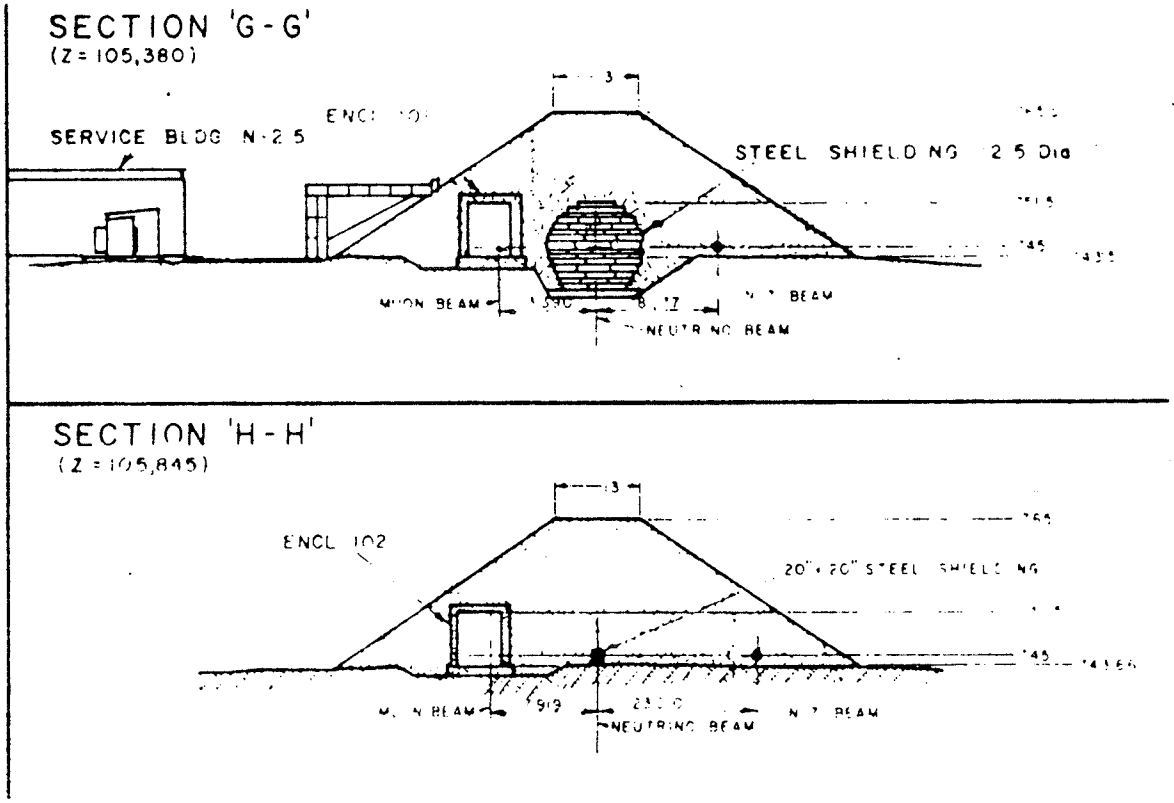

Fig.7 The cross-section of berm at the NW8 area.

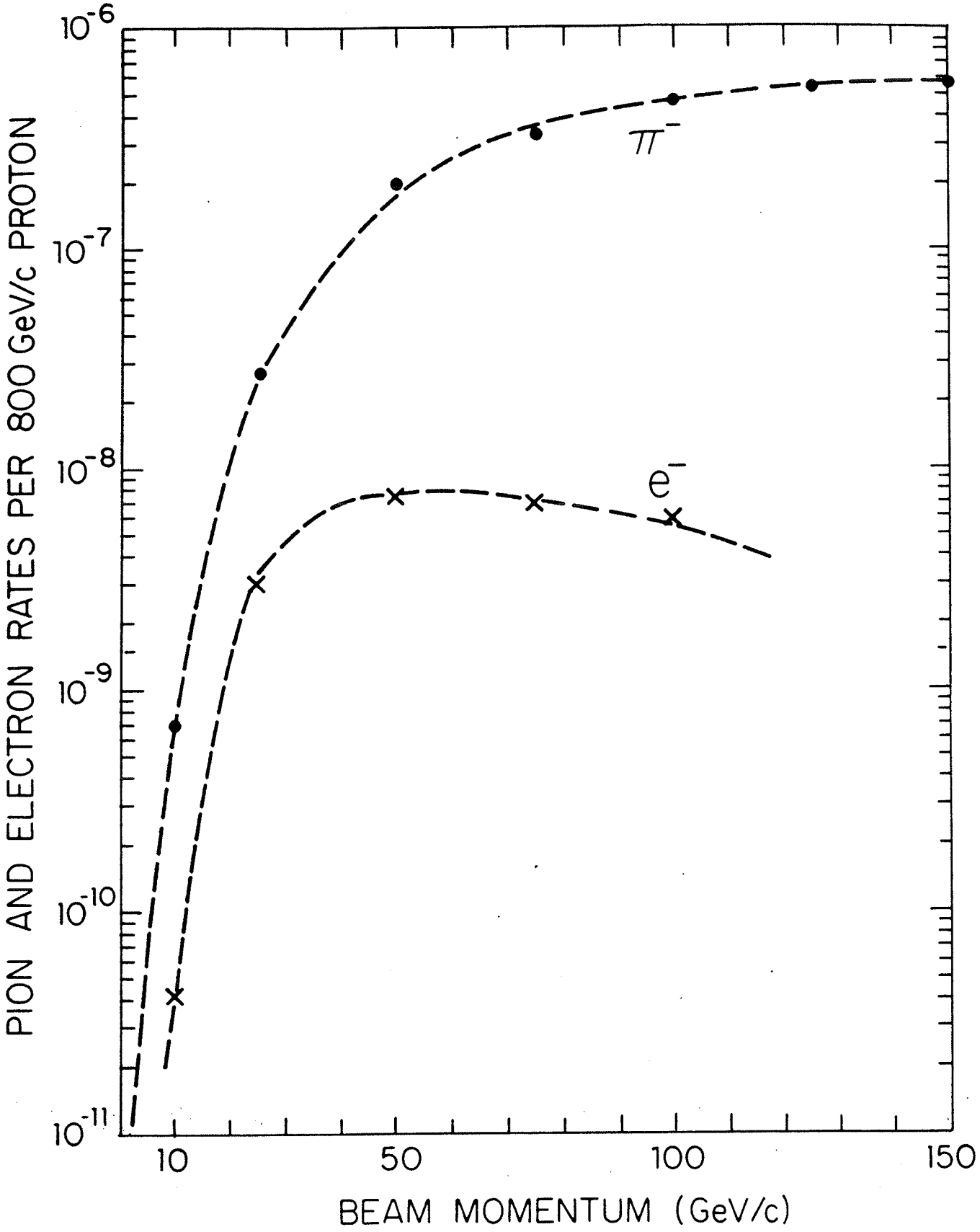

Fig.8 Typical 1980's pion and electron beam rates in the NW beam line.

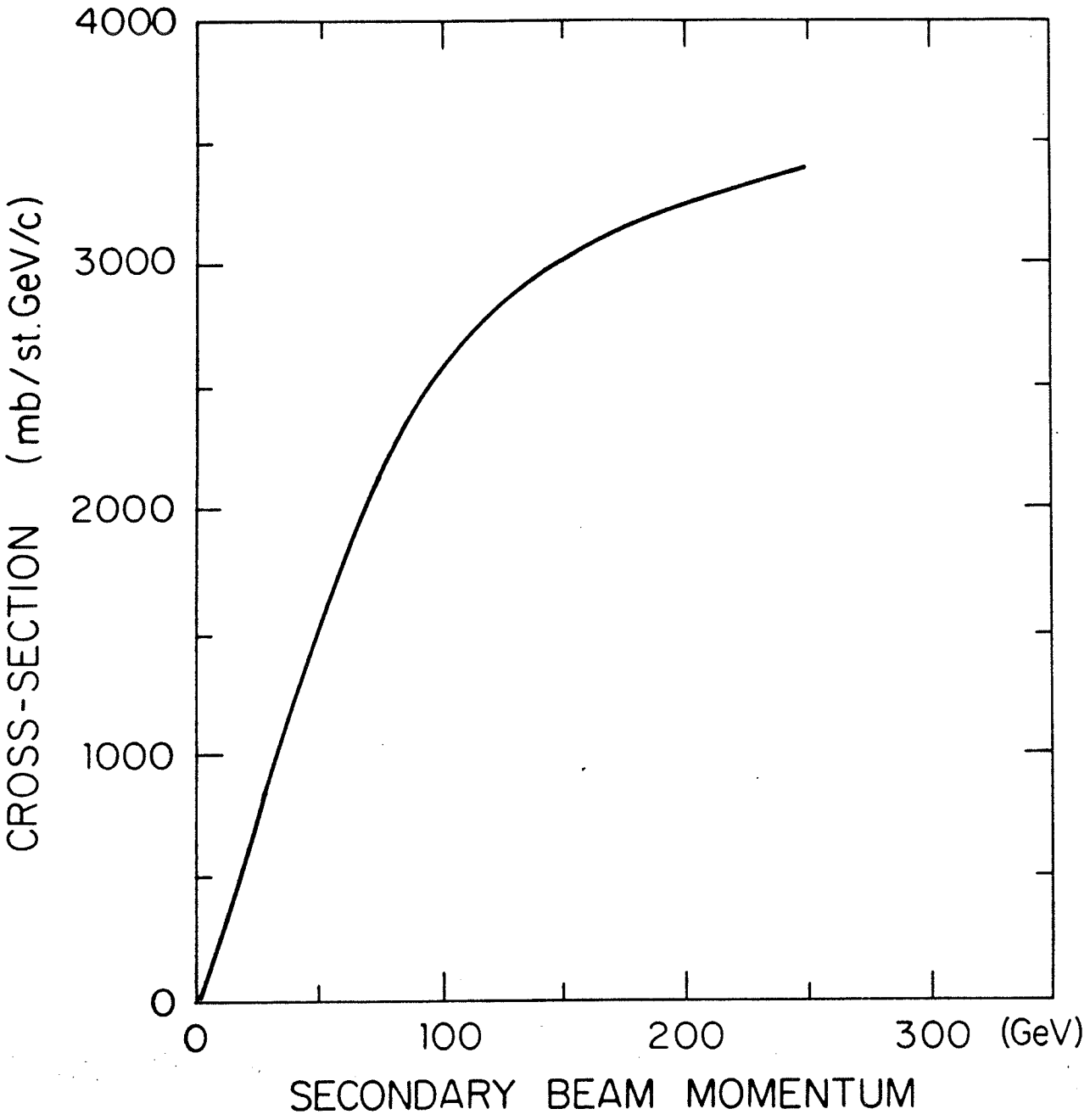

Fig.9 The estimated negative pion production cross-section by the 800 GeV/c protons.

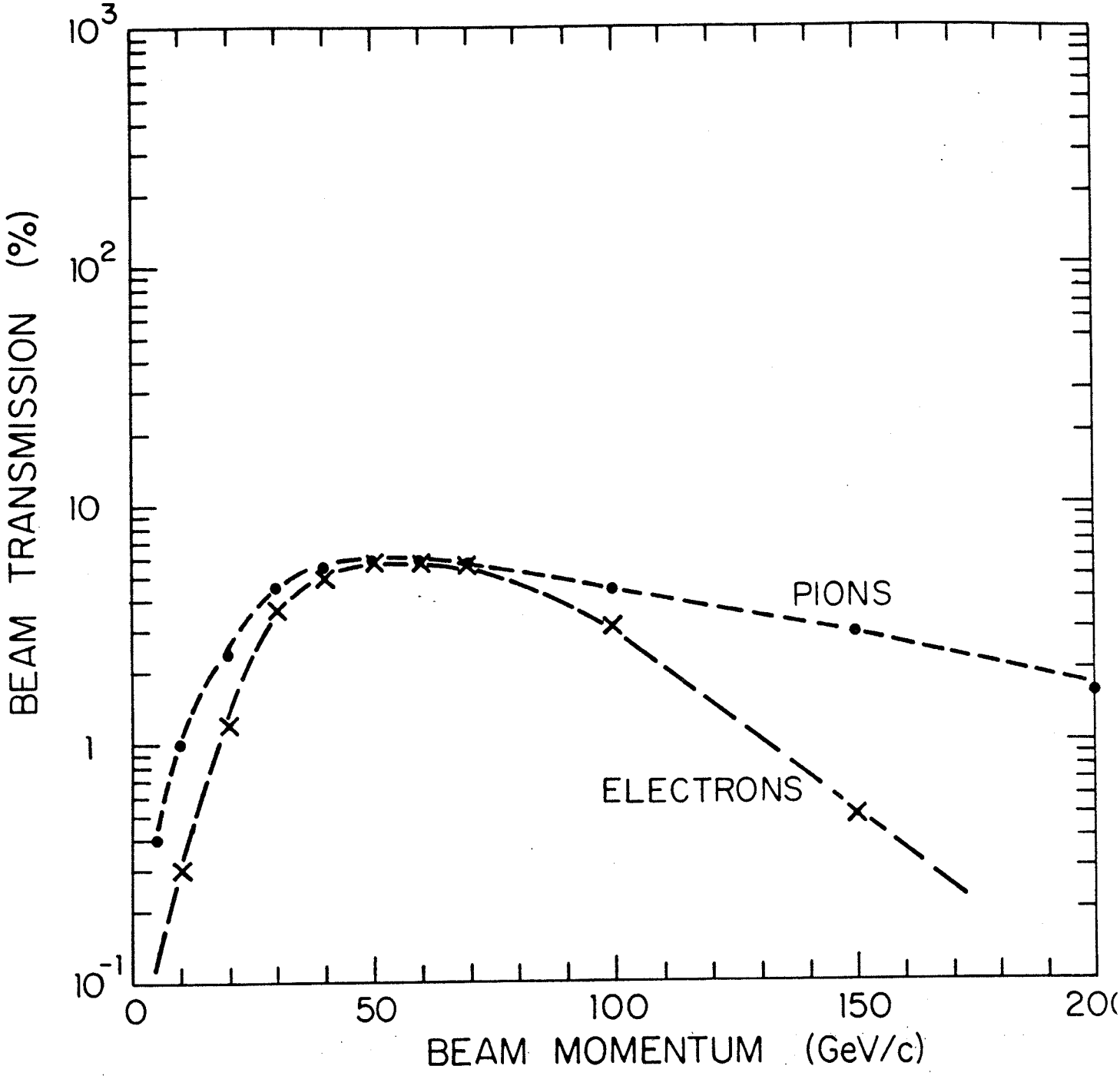

Fig.10 The NW beam line acceptance for negative pions. The electron acceptance was normalized to pion acceptance at 60 GeV/c.

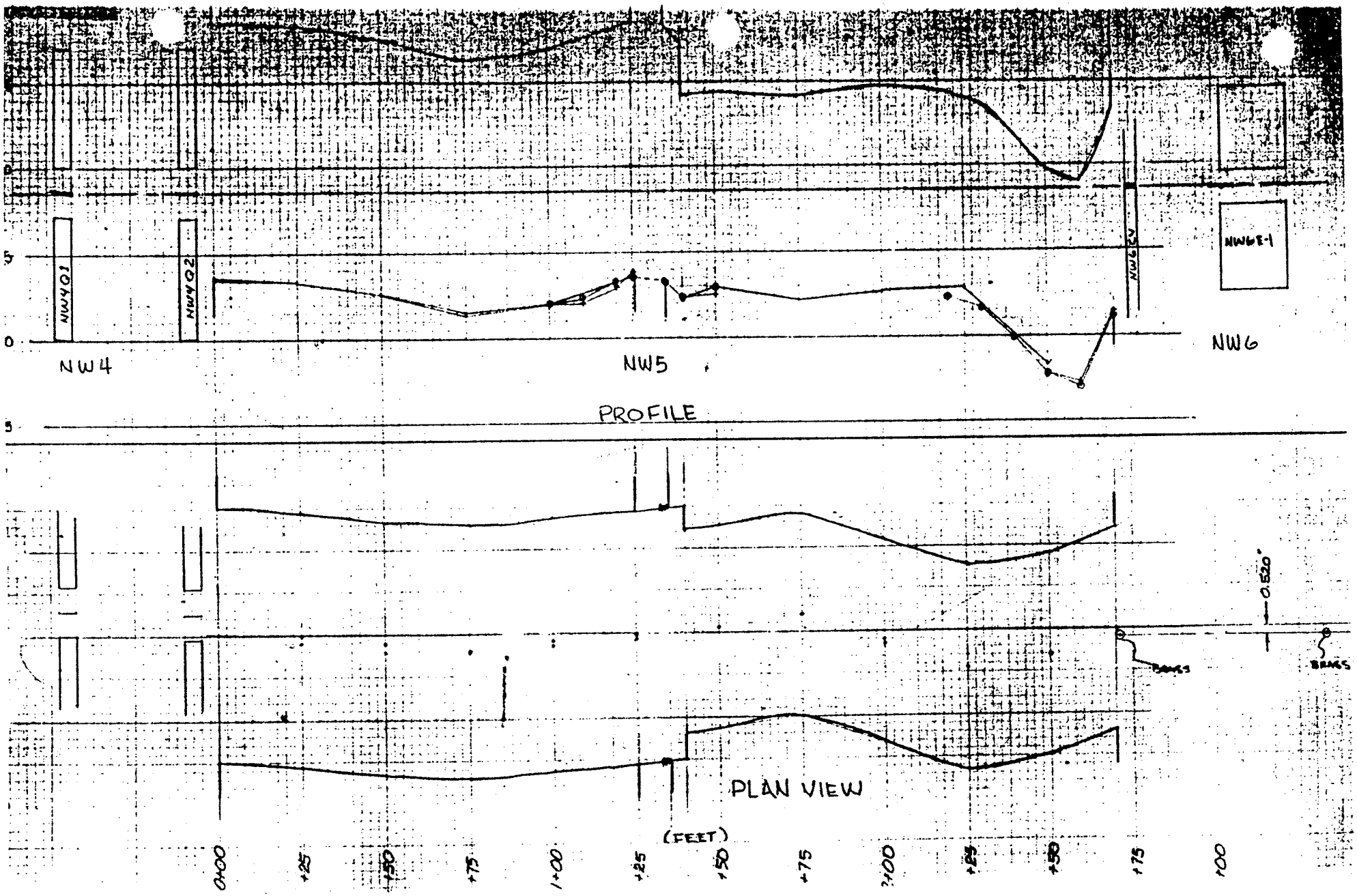

Fig.11 The bent section of the decay pipe in the NW5 enclosure

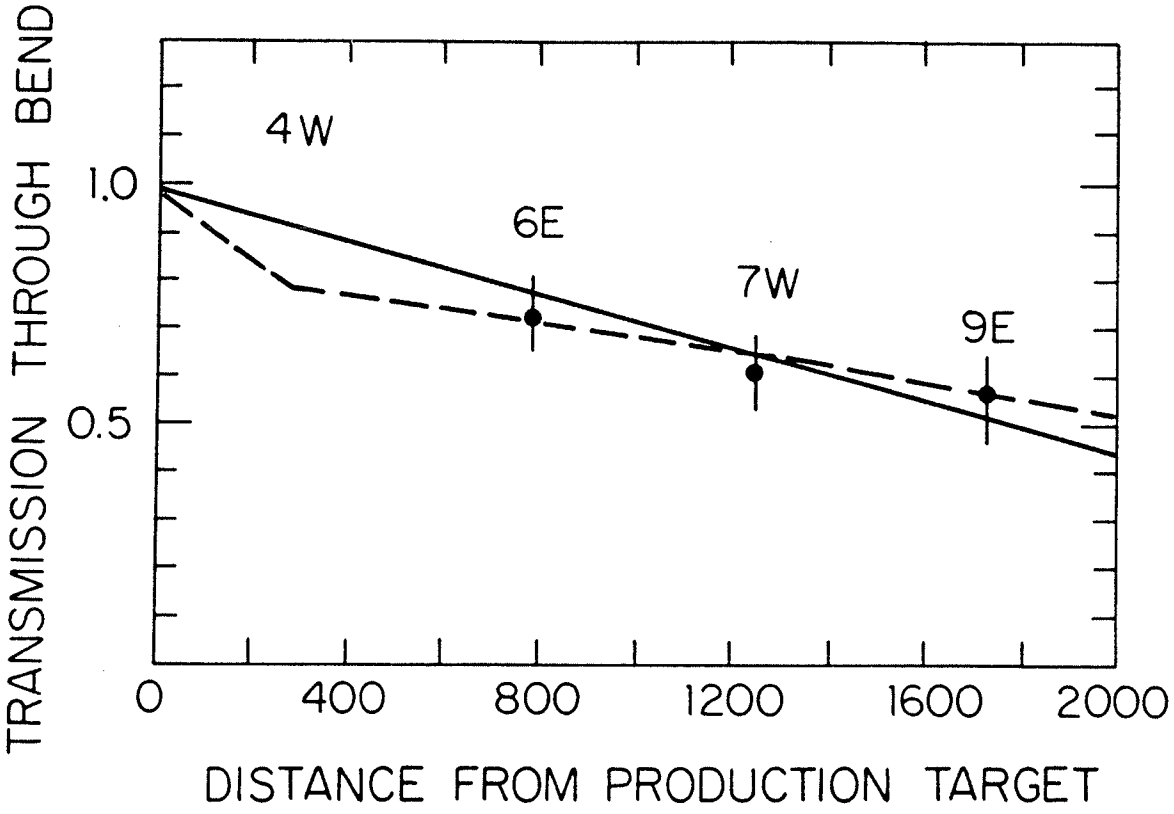

Fig.12 The secondary, 100 GeV/c pion beam intensity loss on bends. The solid and dashed lines indicate two possibilities of the beam intensity loss on bends.

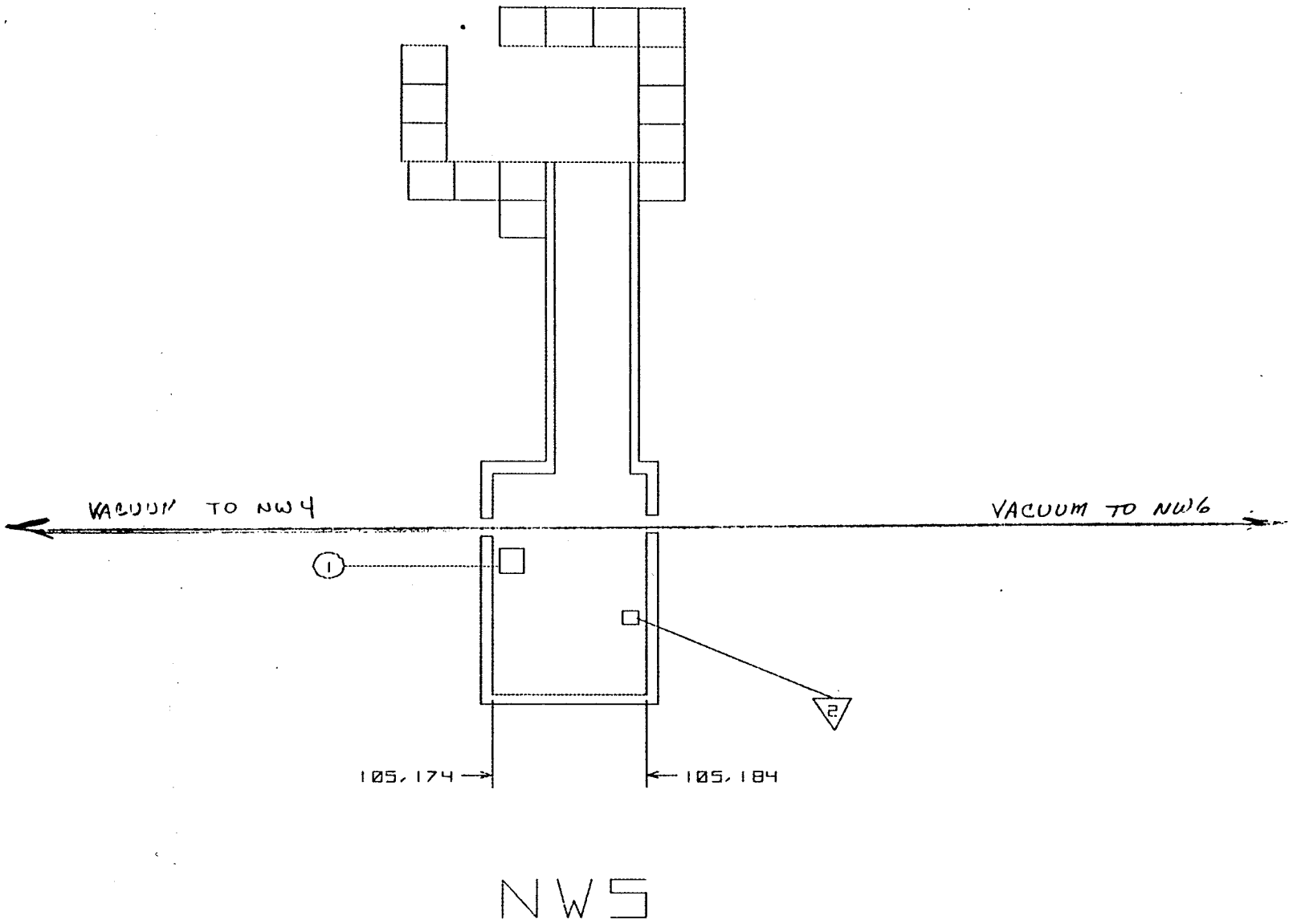

Fig.13a The NW beam pipe windows and instrumentation in area of NW5

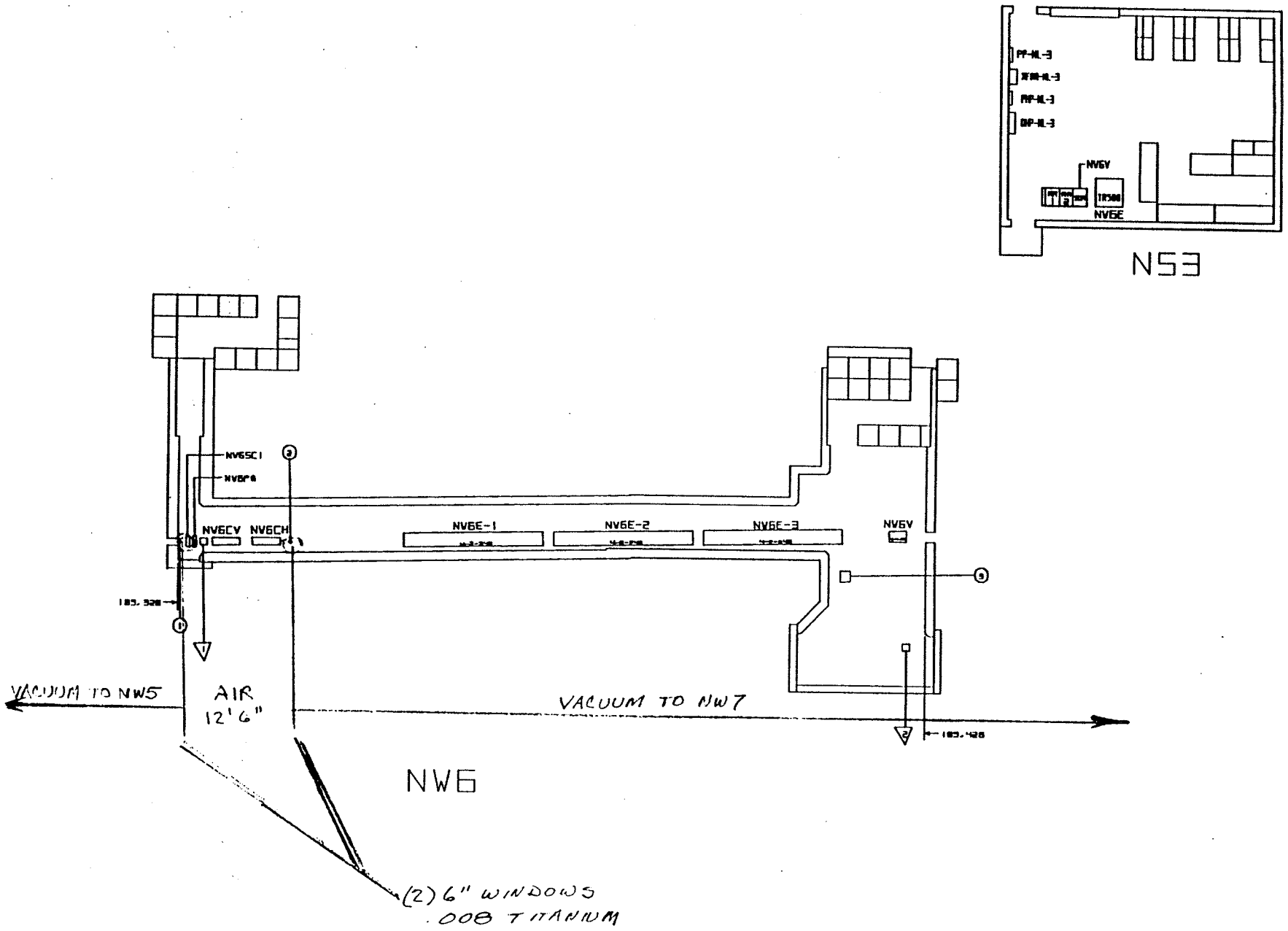

Fig.13b The NW beam pipe windows and instrumentation in area of NW6

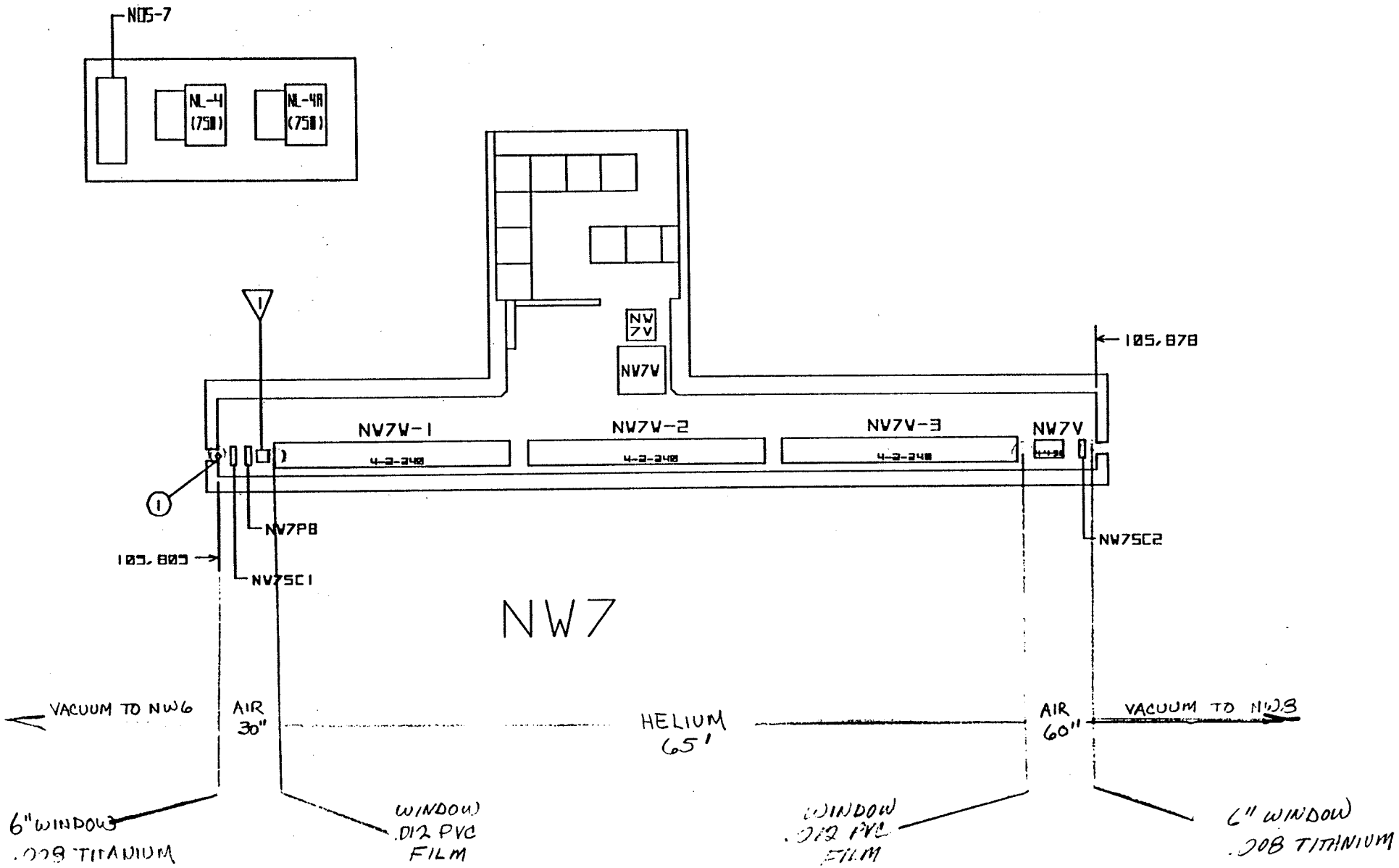

Fig.13c The NW beam pipe windows and instrumentation in area of NW7

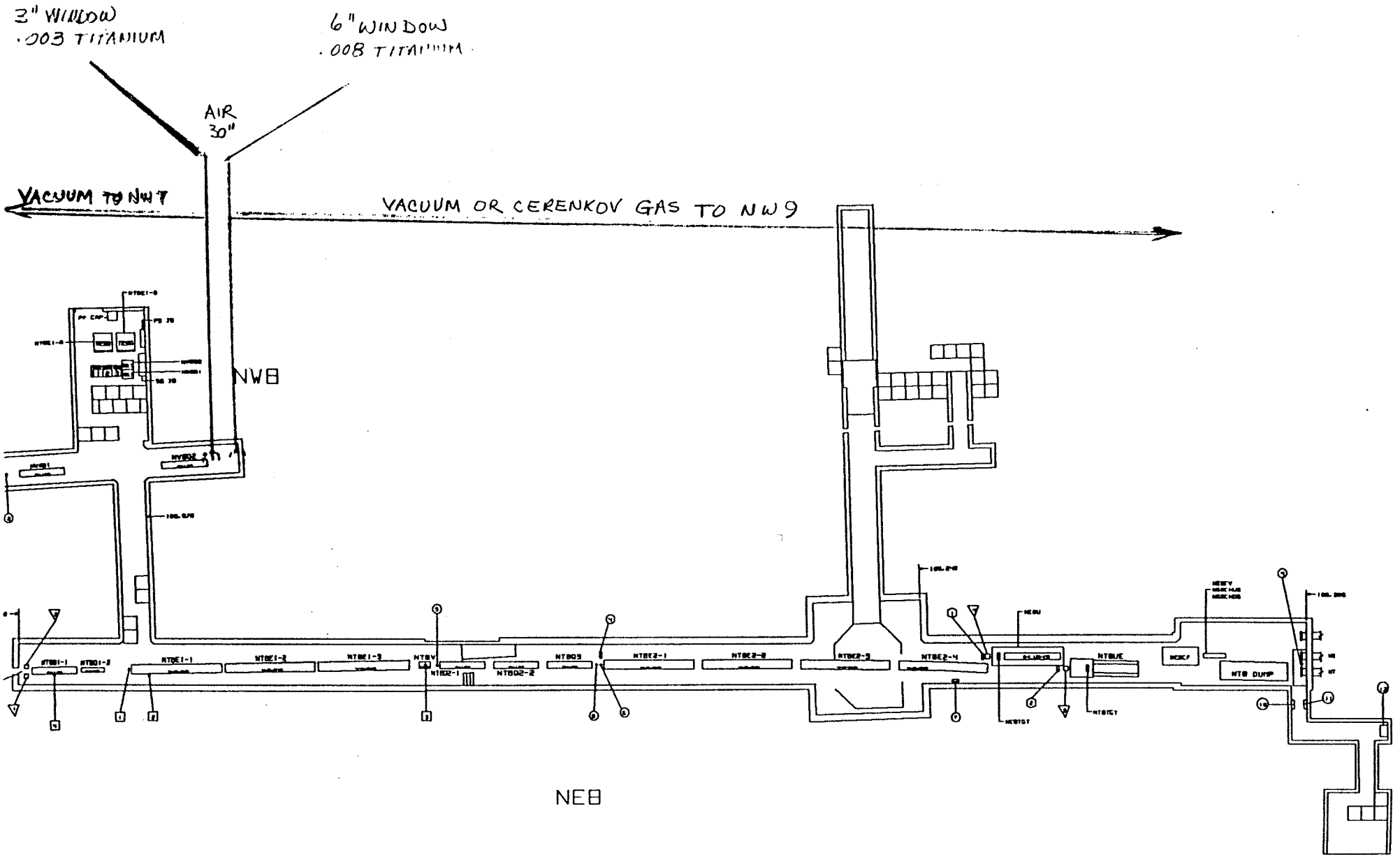

Fig.13d The NW beam pipe windows and instrumentation in area of NW8

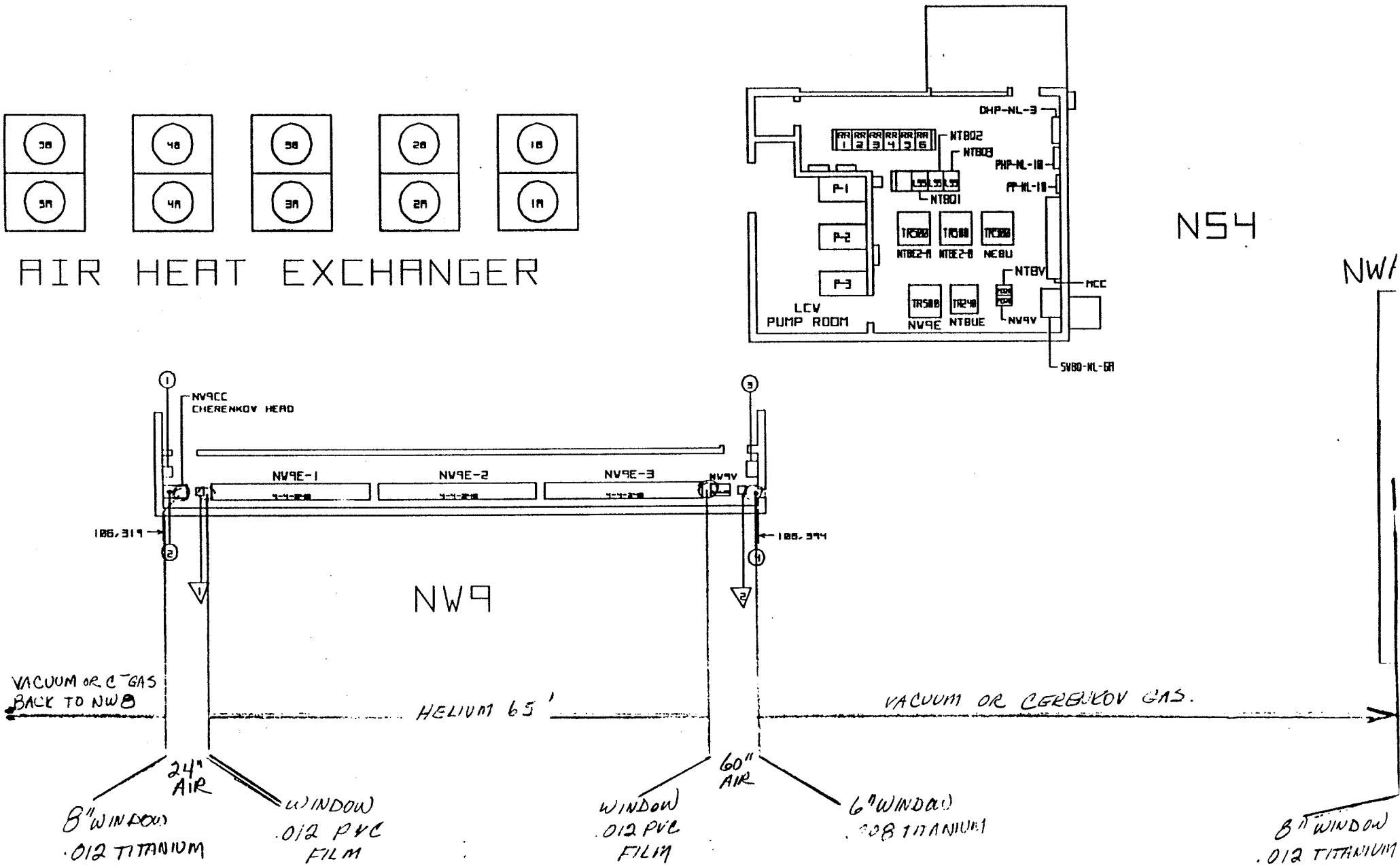

Fig.13e The NW beam pipe windows and instrumentation in area of NW9

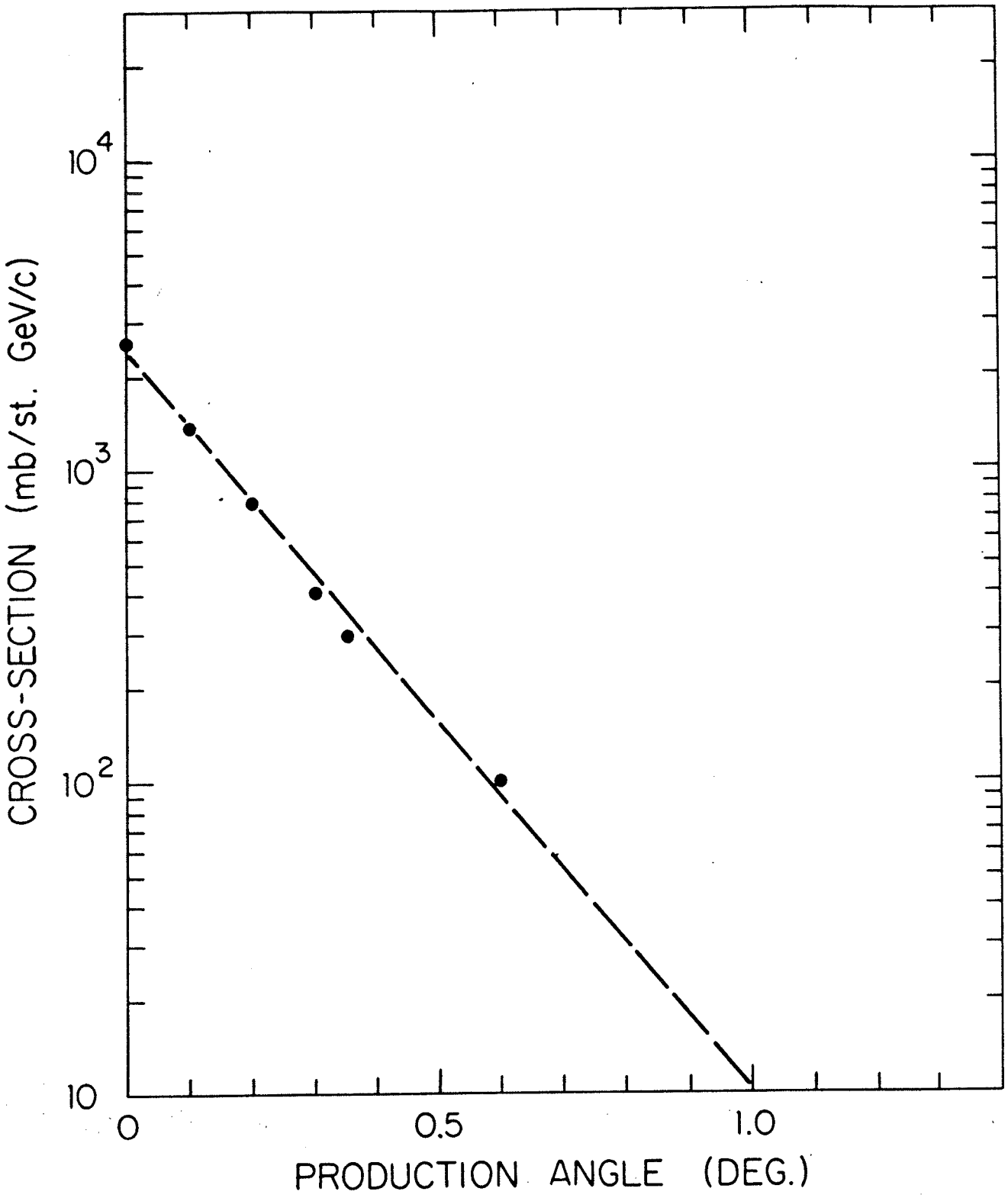

Fig.14 Production cross-section of 100 GeV/c pions by 800 GeV/c protons as a function of the scattering angle.

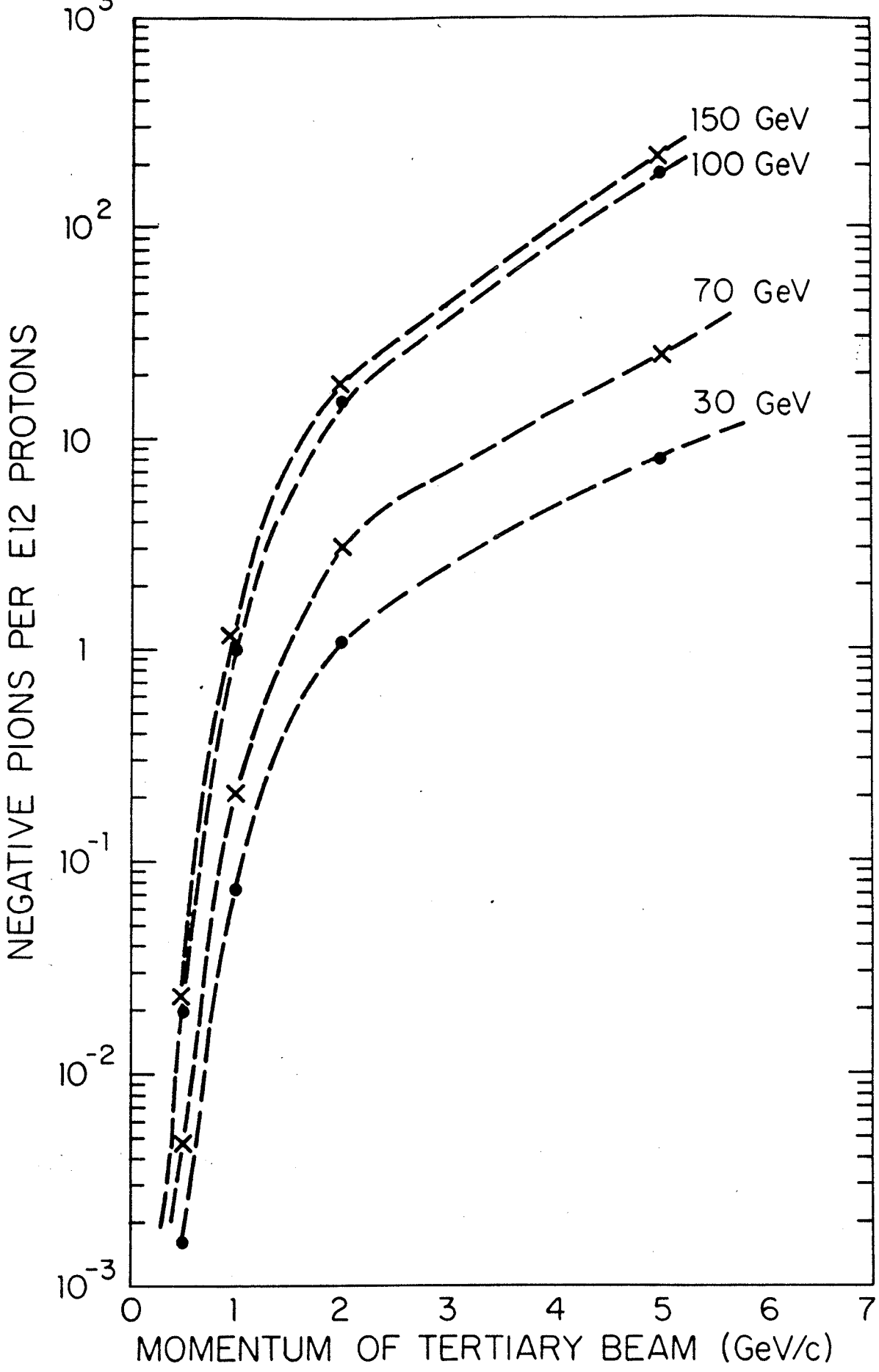

Fig.15 Production rate of the tertiary beams by 30, 70, 100 and 150 GeV/c secondary negative pion beam.

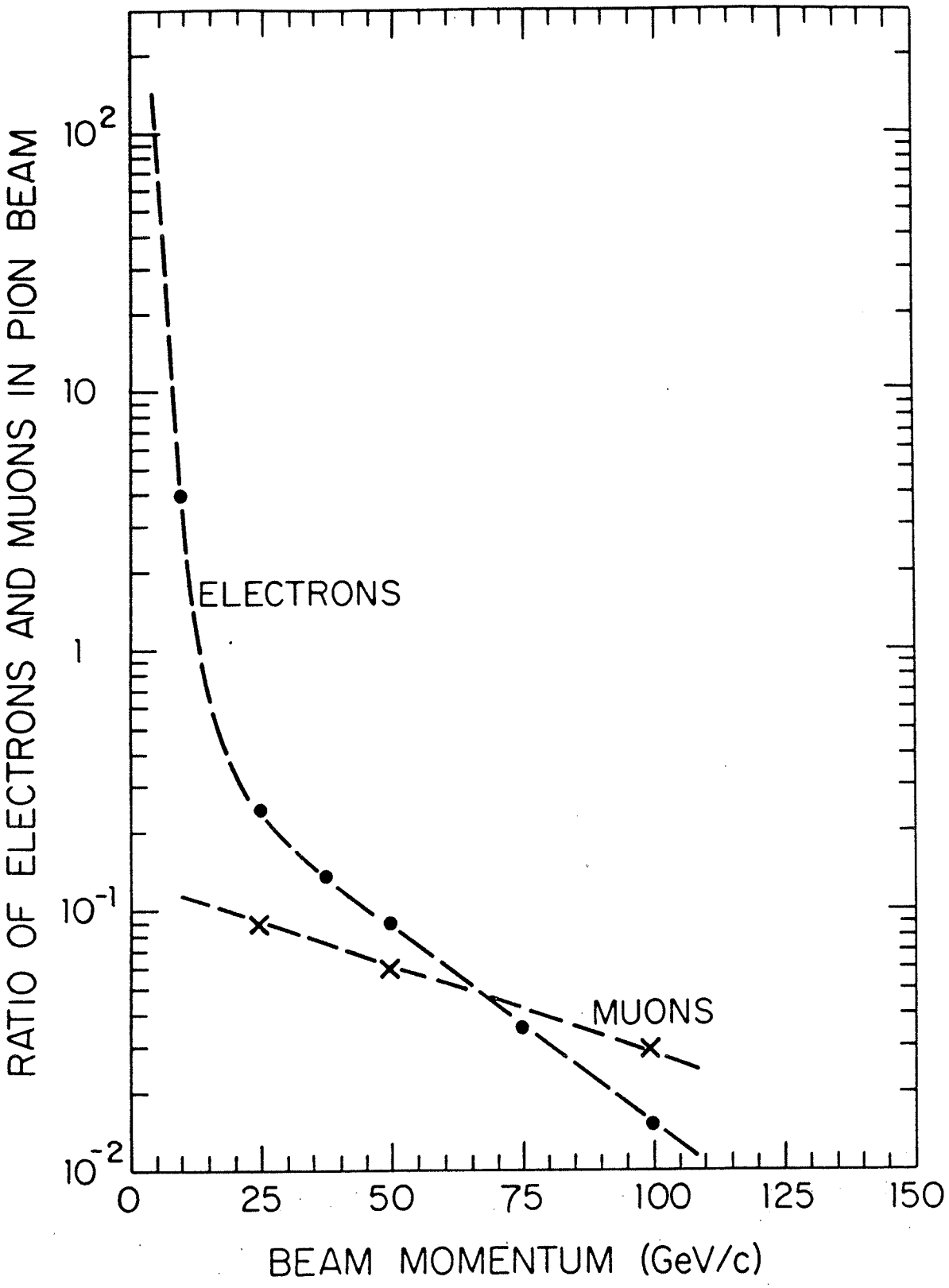

Fig.16 The electron and muon contents of the secondary pion beams.

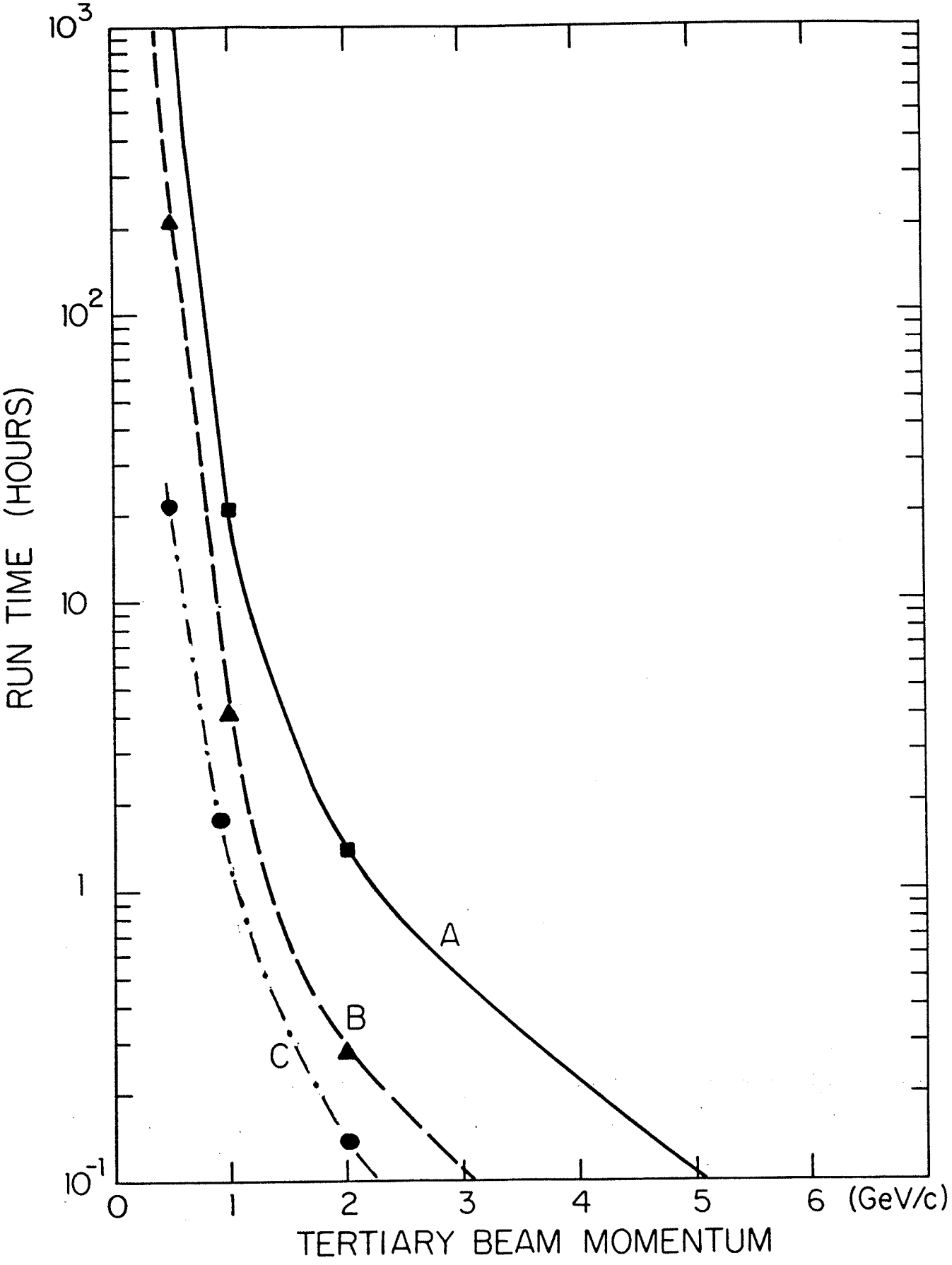

Fig.17 The projected running time for 1000 (A) and 200 (B) events of the low momentum negative pions. The curve C shows running time for 200 hadronic (pions + protons) events. All times are for tertiary beam produced in NW8.